Effective Charge Transfer Distances in Cyanide-Bridged Mixed-Valence Transition Metal Complexes

Gerold U. Bublitz,[†] William M. Laidlaw,[‡] Robert G. Denning,[‡] and Steven G. Boxer*,[†]

Contribution from the Department of Chemistry, Stanford University, Stanford, California 94305-5080, and the Inorganic Chemistry Laboratory, University of Oxford, South Parks Road, Oxford OX1 3QR, UK

Received February 9, 1998

Abstract: Stark (electroabsorption) spectroscopy can provide quantitative information on the change in dipole moment and polarizability for an electronic transition. In the case of mixed-valence transitions, the change in dipole moment associated with the intervalence charge-transfer band can be used to establish the effective charge-transfer distance required for estimating the intermetallic electronic coupling using Hush theory (Oh; Boxer *J. Am. Chem. Soc.* **1990**, *112*, 8161). Stark spectra are reported for a series of cyanide-bridged complexes with $-Ru^{III}(NH_3)_5$ as the acceptor and different metal/ligand combinations as the donor. The origins of differences between the effective charge-transfer distance based on the intermetallic distance and the dipole moment differences measured by Stark spectroscopy are discussed. The possible difference in the effective charge-transfer distances for spin−orbit states in $[(NC)_5Os^{II}\text{-}CN\text{-}Ru^{III}(NH_3)_5]^-$, recently described by Karki and Hupp (*J. Am. Chem. Soc.* **1997**, *110*, 4070), is reevaluated, and it is shown that these distances are the same within experimental error for these spin−orbit states. These data provide informative examples of methods used to evaluate Stark data and the power of using higher-order Stark spectroscopy (Lao et al. *J. Phys. Chem.* **1995**, *99*, 496) to measure the change in dipole moment for broad and relatively weak transitions often encountered in mixed-valence systems.

Mixed-valence transition metal complexes exhibit a metal-to-metal charge transfer (MMCT) transition in the visible to near-IR region of the spectrum (for reviews see, e.g. refs 1−5). The extent of charge transfer associated with the MMCT process, a critical factor in characterizing electronic interactions, is difficult to obtain quantitatively. For weak coupling between the donor and acceptor metal atoms, the ground state of the complex is valence trapped (Robin-Day class II) with only a small degree of ground-state delocalization. In these cases the electronic coupling matrix element, H_{ab}, can be estimated by using Hush theory:[2,5,6]

$$H_{ab} = (2.06 \times 10^{-2})\frac{\sqrt{\bar{\nu}_{max} \cdot \epsilon_{max} \cdot \bar{\nu}_{1/2}}}{\Delta\mu/e} \qquad (1)$$

where $\bar{\nu}_{max}$, ϵ_{max}, and $\bar{\nu}_{1/2}$ are the peak location, extinction coefficient, and full-width at half-maximum, respectively, of the absorption. $\Delta\mu$ is the change in dipole moment between the ground and excited state and defines the effective charge-transfer distance, $r_{ab} = |\Delta\mu|/e$, where e is the unit of charge.

In the absence of direct measurements of $\Delta\mu$, the metal−metal separation distance has typically been used as the best estimate for r_{ab}. Several years ago, Oh and Boxer demonstrated that effective charge transfer distances of metal-to-ligand, ligand-to-metal, and metal-to-metal charge transfer processes can be obtained directly by Stark or electroabsorption spectroscopy.[7−10] The Stark effect describes the influence of an externally applied electric field on the absorption spectrum of a molecule. Oh and Boxer compared Stark data for $[(NH_3)_5Ru^{II}\text{-}4,4'\text{-bpy-}Ru^{III}(NH_3)_5]^{5+}$ with the Creutz-Taube ion, $[(NH_3)_5Ru^{II}\text{-pyrazine-}Ru^{III}(NH_3)_5]^{5+}$.[8,9] A substantial amount of charge transfer ($f \cdot |\Delta\mu| = 28$ D, corresponding to $52/f$ % of the metal−metal separation distance)[11] was found for the former complex in which the two metal centers are connected by a 4,4′-bipyridine bridge, indicating a mostly localized ground state structure. Little or no charge transfer was observed upon excitation of the Creutz-Taube complex where the two metal centers are connected by a pyrazine bridge. In this case the ground state is effectively

[†] Stanford University.
[‡] University of Oxford.

(1) Allen, G. C.; Hush, N. S. *Prog. Inorg. Chem.* **1967**, *8*, 357−389.
(2) Hush, N. S. *Prog. Inorg. Chem.* **1967**, *8*, 391−444.
(3) Robin, M. B.; Day, P. *Adv. Inorg. Chem. Radiochem.* **1967**, *10*, 247.
(4) Creutz, C. *Prog. Inorg. Chem.* **1983**, *30*, 1−73.
(5) Crutchley, R. J. *Adv. Inorg. Chem.* **1994**, *41*, 273−325.
(6) Cave, R. J.; Newton, M. D. *Chem. Phys. Lett.* **1996**, *249*, 15−19.
(7) Oh, D.; Boxer, S. G. *J. Am. Chem. Soc.* **1989**, *111*, 1130−1131.
(8) Oh, D. H.; Boxer, S. G. *J. Am. Chem. Soc.* **1990**, *112*, 8161−8162.
(9) Oh, D. H.; Sano, M.; Boxer, S. G. *J. Am. Chem. Soc.* **1991**, *113*, 6880−6890.
(10) Oh, D. H., Ph.D. Thesis, Stanford University, 1991.

(11) f is the local field correction, describing the difference in electric field strength, F, at the position of the molecule from that of the externally applied field, F_{ext}: $F = f \cdot F_{ext}$. f can be modeled by using the dielectric constant ϵ of the solvent (see: Böttcher, C. J. F. *Theory of Electric Polarization*, 2nd ed.; Elsevier: Amsterdam, 1973; Vol. 1). The most simple approach employs the picture of a spherical cavity created in the solvent by the solute and predicts $f = 3\epsilon/(2\epsilon + 1)$. Including the dielectric constant of the solute molecule and adjusting the shape of the cavity to approximate that of the molecule usually lead to smaller predicted values of f, i.e., values closer to unity. An approach based on bulk dielectric measurements (e.g. via measurements of the sample capacitance) might fail if the solvent is locally ordered in the vicinity of the chromophore, as has been recently suggested (Bublitz, G. U.; Boxer, S. G. *J. Am. Chem. Soc.* In press). For a given solvent this ordering depends on the dipolar properties of the solute. Differences in the partial charges present at the ligand−solvent (i.e. outer sphere−inner sphere) interface might lead to different values of f for different compounds even if their geometric proportions are similar. To separate this factor from the experimental results we report all parameters determined by Stark spectroscopy in terms of f.

S0002-7863(98)00453-3 CCC: $15.00
Published on Web 06/05/1998

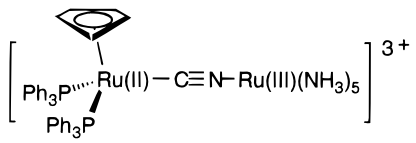

1

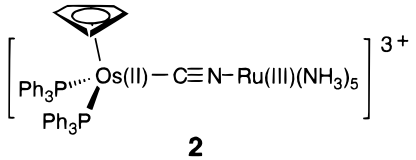

2

3

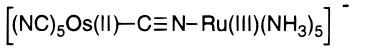

4

Figure 1. Chemical structures of the studied mixed-valence transition metal complexes.

delocalized, that is, the appropriate description is $[(NH_3)_5Ru^{2.5}$-pyrazine-$Ru^{2.5}(NH_3)_5]^{5+}$ (Class III in the Robin-Day classification).

More generally, the same set of issues arises for organic donor−acceptor compounds or for any system where electron transfer occurs. For example, we recently reported Stark data for a series of donor−acceptor polyenes prepared for studies of the origin of second-order nonlinear optical properties,[12,13] and it has recently been shown that mixed-valence complexes likewise exhibit strong optical nonlinearity,[14] as predicted from the Stark results.[9] We have also found that weak interactions between chromophores that participate in long-distance electron transfer leads to unusual and informative Stark and higher-order Stark (see below) line shapes.[15]

In the present paper we investigate the group of cyanide-bridged mixed-valence complexes **1**−**4** shown in Figure 1. Compound **3** is isoelectronic and isostructural to $[(NC)_5Fe^{II}$-CN-$Os^{III}(NH_3)_5]^-$ for which Stark data have recently been reported.[16] In contrast to the other compounds, the metal atom on the donor side of **3** is a group VI transition metal atom. All compounds are d^6−d^5 transition metal complexes. Stark spectra of **4** were recently reported by Karki and Hupp.[17] We have reexamined compound **4** to investigate the possibility of orbital-specific charge-transfer characteristics and reach rather different conclusions than those reported by Karki and Hupp.

Experimental Section

The setup for recording Stark spectra has been described in detail elsewhere.[12] Briefly, light from a tungsten−halogen lamp was passed through a 0.22 m single monochromator, horizontally polarized, focused through the sample, and detected with an amplified silicon photodiode. The sample consists of two microscope slides coated with a transparent ITO electrode and held apart by a Mylar spacer with a nominal thickness of 25 μm. The actual thickness of the empty sample cuvette was determined interferometrically. An AC electric field was supplied by a custom built high-voltage power supply, amplifying an externally supplied sinusoidal wave. Samples were immersed in liquid nitrogen in a dewar fitted with strain free quartz windows. The angle χ between the direction of the externally applied field and the electric vector of the polarized light was varied by rotating the Stark sample about the vertical axis.

Conventional (2ω, see below) Stark spectra were obtained by lock-in detection at twice the fundamental modulation frequency ω of the externally applied AC electric field. Higher order Stark spectra (HOSS) were obtained by using lock-in detection at four times the fundamental frequency (4ω, see below). The changes in absorption, ΔA, due to application of the electric field were calculated from the experimentally determined Stark signal (ΔI) and the direct output of the photodiode (I): $(\Delta A(2\omega) = (2\sqrt{2}/\ln 10)\cdot(\Delta I(2\omega)/I)$ and $(\Delta A(4\omega) = (8\sqrt{2}/\ln 10)\cdot(\Delta I(4\omega)/I)$. Absorption spectra were taken on the same setup as the Stark spectra as well as on a Perkin-Elmer Lambda 12 spectrophotometer. Both gave identical spectra.

Compounds **1**−**4** were synthesized as described in the literature.[18−20] For the Stark and absorption experiments, compounds **1**−**3** were dissolved in a 1:1 acetone:EtOH solvent mixture. To study compound **4** under identical conditions as previously reported,[17] it was dissolved in a 1:1 glycerol−water solvent mixture. Solutions of compound **1** did not have sufficient optical density to obtain HOSS.

Method of Analysis

For an isotropic, immobilized sample placed in an electric field, $\Delta\mu$ will lead to a broadening and $\Delta\alpha$ (the difference polarizability between ground state and excited state) will lead to a shift of the absorption spectrum. These two effects combine to give a Stark spectrum line shape (ΔA = field-on minus field-off) that is a weighted sum of the second and first derivative of the absorption spectrum, respectively.[21] Typically these spectra are obtained by modulating the electic field at frequency ω and detecting the signal at 2ω, and ΔA depends quadrically on the field strength. We recently introduced a new technique called higher-order Stark spectroscopy (HOSS) that measures the higher even-harmonic responses (4ω, 6ω, etc.) of the absorption to the applied field; ΔA depends on the fourth, sixth, etc. power of the field.[22] An important feature of HOSS data is that $\Delta\mu$ can be determined accurately for cases where the absorption and absorption derivatives cannot be determined precisely (e.g., for weak absorbers, broad lines, or overlapping absorption features). For a detailed review of both techniques see ref 12.

The conventional (2ω) Stark response can be expressed in terms of derivatives of the absorption spectrum:[12,23]

$$\Delta A(2\omega, \bar{\nu}) = F^2\left\{A_\chi A(\bar{\nu}) + \frac{B_\chi}{15hc}\bar{\nu}\frac{\mathrm{d}}{\mathrm{d}\bar{\nu}}\left(\frac{A(\bar{\nu})}{\bar{\nu}}\right) + \frac{C_\chi}{30h^2c^2}\bar{\nu}\frac{\mathrm{d}^2}{\mathrm{d}\bar{\nu}^2}\left(\frac{A(\bar{\nu})}{\bar{\nu}}\right)\right\} \quad (2)$$

with

(12) Bublitz, G. U.; Boxer, S. G. *Annu. Rev. Phys. Chem.* **1997**, *48*, 207−242.
(13) Bublitz, G. U.; Ortiz, R.; Runser, C.; Fort, A.; Barzoukas, M.; Marder, S. R.; Boxer, S. G. *J. Am. Chem. Soc.* **1997**, *119*, 2311−2312.
(14) Laidlaw, W. M.; Denning, R. G.; Verbiest, T.; Chauchard, E.; Persoons, A. *Nature* **1993**, *363*, 58−59.
(15) Zhou, H.; Boxer, S. G. *J. Phys. Chem.* Submitted for publication.
(16) Karki, L.; Lu, H. P.; Hupp, J. T. *J. Phys. Chem.* **1996**, *100*, 15637−15639.
(17) Karki, L.; Hupp, J. T. *J. Am. Chem. Soc.* **1997**, *119*, 4070−4073.
(18) Laidlaw, W. M.; Denning, R. G. *J. Chem. Soc., Dalton Trans.* **1994**, 1987−1994.
(19) Laidlaw, W. M.; Denning, R. G. *Polyhedron* **1994**, *13*, 2337−2342.
(20) Laidlaw, W. M.; Denning, R. G. *Polyhedron* **1994**, *13*, 1875−1880.
(21) Additionally, electric field induced changes of the absorption intensity lead to a Stark spectrum with a line shape similar to that of the absorption spectrum (zeroth derivative line shape). All three effects can occur simultaneously, and the experimentally determined Stark spectrum is analyzed in terms of the three derivative components (zeroth, first, and second derivative of the absorption spectrum).
(22) Lao, K.; Moore, L. J.; Zhou, H.; Boxer, S. G. *J. Phys. Chem.* **1995**, *99*, 496−500.
(23) Liptay, W., In *Excited States*; Lim, E. C., Ed.; Academic Press: New York, 1974; pp 129−229.

$$B_\chi = \frac{5}{2}\mathrm{Tr}(\Delta\alpha) + (3\cos^2\chi - 1)\left(\frac{3}{2}\Delta\alpha_m - \frac{1}{2}\mathrm{Tr}(\Delta\alpha)\right) + (A\cdot\Delta\mu \text{ cross-term contributions}) \quad (3)$$

and

$$C_\chi = |\Delta\mu|^2\cdot[5 + (3\cos^2\chi - 1)(3\cos^2\zeta_A - 1)] \quad (4)$$

Here χ is the experimental angle between the externally applied field and the polarization of the incident light, ζ_A is the internal angle between $\Delta\vec{\mu}$ and the transition moment $\vec{m}$, and $\Delta\alpha_m$ is the component of the polarizability change along the direction of the transition moment (i.e. $\Delta\alpha_m = (\vec{m}\Delta\alpha\vec{m})/|\vec{m}|^2$). A_χ, the zeroth derivative component, is linked to the electric-field-induced change of the transition dipole moment and is usually small compared to the other two components, B_χ and C_χ. The first derivative component, B_χ, has contributions from two sources, $\Delta\alpha$ and cross-terms between A and $\Delta\mu$. The latter are often ignored, and $\Delta\alpha$ is calculated directly from B_χ. The second derivative component, C_χ, is directly linked to $|\Delta\mu|$, the amount of charge transfer upon excitation.

The expression for 4ω-HOSS is similar to eq 2, but now the Stark response corresponds to a sum of zeroth through fourth derivatives of the absorption spectrum:

$$\Delta A(4\omega, \bar{\nu}) = F^4\cdot\left(A_\chi^{4\omega}\cdot A(\bar{\nu}) + \frac{B_\chi^{4\omega}}{35hc}\bar{\nu}\frac{d}{d\bar{\nu}}\left(\frac{A(\bar{\nu})}{\bar{\nu}}\right) + \frac{C_\chi^{4\omega}}{70h^2c^2}\bar{\nu}\frac{d^2}{d\bar{\nu}^2}\left(\frac{A(\bar{\nu})}{\bar{\nu}}\right) + \frac{D_\chi^{4\omega}}{210h^3c^3}\bar{\nu}\frac{d^3}{d\bar{\nu}^3}\left(\frac{A(\bar{\nu})}{\bar{\nu}}\right) + \frac{E_\chi^{4\omega}}{840h^4c^4}\bar{\nu}\frac{d^4}{d\bar{\nu}^4}\left(\frac{A(\bar{\nu})}{\bar{\nu}}\right)\right) \quad (5)$$

with

$$E_\chi^{4\omega} = |\Delta\mu|^4\cdot[7 + 2(3\cos^2\chi - 1)(3\cos^2\zeta_A - 1)] \quad (6)$$

so that again the highest (fourth) derivative component is related only to the amount of charge transfer, $|\Delta\mu|$.

For large values of $\Delta\mu$, the second derivative coefficient C_χ and fourth derivative coefficient $E_\chi^{4\omega}$ dominate the 2ω- and 4ω-Stark response, respectively. In this case the line shape of the 4ω-HOSS is predicted to resemble that of the $\bar{\nu}$-weighted second derivative of the 2ω-Stark spectrum, and $|\Delta\mu|$ can be calculated from the ratio of these two spectra:

$$\frac{\Delta A_{\Delta\mu}(4\omega, \bar{\nu})}{\bar{\nu}\frac{\partial^2}{\partial\bar{\nu}^2}\left(\frac{\Delta A_{\Delta\mu}(2\omega, \bar{\nu})}{\bar{\nu}}\right)} = F^2\cdot\frac{[7 + 2(3\cos^2\chi - 1)(3\cos^2\zeta_A - 1)]}{28h^2c^2[5 + (3\cos^2\chi - 1)(3\cos^2\zeta_A - 1)]}\cdot|\Delta\mu|^2 \quad (7)$$

The proportionality factor on the right-hand side of eq 7 depends only on the field strength F and the angle χ, both experimental parameters, and on the angle ζ_A between $\Delta\vec{\mu}$ and $\vec{m}$, which can be measured, so this ratio of experimental data provides an independent approach for obtaining $|\Delta\mu|$.

The assumptions underlying eqs 2−6 are believed to be quite robust but do not cover all interactions affecting a molecule in solid solution.[12] The major limitation that will give rise to deviations between data and model originates in the interaction of the polarizability difference, $\Delta\alpha$, of a compound with the electric field created by the solvent matrix surrounding it. This matrix field induces a dipole moment, $\vec{\mu}_{ind} = \alpha\cdot\vec{F}_{matrix}$, which adds to the molecule's intrinsic, permanent dipole moment, $\vec{\mu}_0$, to give $\vec{\mu} = \vec{\mu}_0 + \vec{\mu}_{ind}$. An intrinsic difference in polarizability for the molecule thus can lead to an induced difference dipole moment between ground and excited state, $\vec{\mu}_{ind} = \Delta\alpha\cdot\vec{F}_{matrix}$. If the magnitude of $\Delta\mu_{ind}$ does not change across the absorption spectrum, this factor will have no effect on the analysis of the Stark spectrum, and the experimentally determined $|\Delta\mu|$ will just be the sum of the intrinsic and induced difference dipole moments. However, the same factors that contribute to inhomogeneous broadening of the absorption spectrum, i.e., a spread in matrix field strength, can also lead to a spread in $\Delta\mu_{ind}$ across the inhomogeneously broadened spectrum. This is not taken into account when the Stark data are analyzed in terms of the derivatives of the inhomogeneous absorption band, so (typically) small deviations between Stark data and the fitting model based on eqs 2−6 are expected.[24]

Table 1. Results of the Analysis of the Stark Spectra for Compounds **1**−**4**

	conventional (2ω) Stark spectra			
compd	A_χ [10^{-20} m^2/V^2]	$\Delta\alpha\cdot f^{2\,a}$ [Å^3]	$\lvert\Delta\mu\rvert\cdot f^b$ [D]	4ω HOSS $\lvert\Delta\mu\rvert\cdot f^b$ [D]
1	5	550	21	*c*
2	7	400	23	24.5
3	8	1000	28	31
4	7	525	24	22

[a] Neglecting $A\Delta\mu$ cross-term contributions. Estimated experimental error ±40%. [b] Assuming $\zeta_A = 0°$. Estimated experimental error ±15%. [c] Not determined.

Results

The Stark spectra of compounds **1**−**4** are shown in Figures 2−5. The absorption and conventional (2ω) Stark spectra of all compounds were scaled to a peak absorption of unity and a field strength of 1 MV·cm^{-1} to facilitate comparisons. The HOSS and $\bar{\nu}$-weighted second derivatives of the 2ω-Stark spectra shown for **2**−**4** were scaled to a field strength of 1 MV·cm^{-1} by using the F^4 and F^2 field dependencies of the signals, respectively. All spectra were obtained at $\chi = 90°$, except for **4**, where $\chi = 65°$ for better comparison with the results in ref 17. Table 1 lists the results of the simultaneous best fit of the absorption and 2ω-Stark spectra to eq 2 for all four compounds. The zeroth, first, and second derivative fitting components from which these numbers were extracted are also shown in Figures 2−5. All 2ω-Stark spectra are clearly dominated by the second derivative component, with relatively small first derivative and only minor zeroth derivative contributions. Accordingly the relative error of the $|\Delta\mu|$ values reported in Table 1 is smaller than that of the $\Delta\alpha$ values. For **2**−**4** the values of $|\Delta\mu|$ which were obtained from the comparison of the HOSS with the derivatives of the 2ω-Stark spectra (cf. eq 7) are also listed in Table 1. The noise of the 4ω-HOSS data is similar to that of the 2ω-Stark spectra; however, the HOSS signal is smaller by a factor of about 100.

The angle ζ_A between the difference dipole and the transition dipole moment can be determined directly from 2ω-Stark data obtained at different experimental angles χ if the Stark response is dominated by $\Delta\mu$ (cf. eq 4).[25] Although this is the case for **1**−**4**, there are uncertainties in the angle adjustment, the magnitude of ΔA is rather small due to the low optical density, and the refractive index of the low-temperature solvents is not known exactly. Taken together these limitations give quite a large error in the value of ζ_A. Within the experimental uncertainty, the data for all four compounds yield values for ζ_A that are close to zero, that is, the transition moment, which is expected to lie along the intermetallic axis, and the direction of charge displacement accompanying the MMCT excitation is

(24) For example, if a molecule has a moderately large value of $\Delta\alpha$ = 500 Å^3, a spread of 1 MV·cm^{-1} in the matrix field strength across the inhomogeneously broadened spectrum will cause a spread of 1.7 D in $\Delta\mu$.

(25) The externally set experimental angle, θ_1, is adjusted by using Snell's law, $n_1 \sin\theta_1 = n_2 \sin\theta_2$ (where $n_1 = 1.205$ is the refractive index of the liquid nitrogen and n_2 that of the sample). $\chi = 90° - \theta_2$. The Stark data are also corrected for the increased path length (i.e. increased absorption) as χ increases.

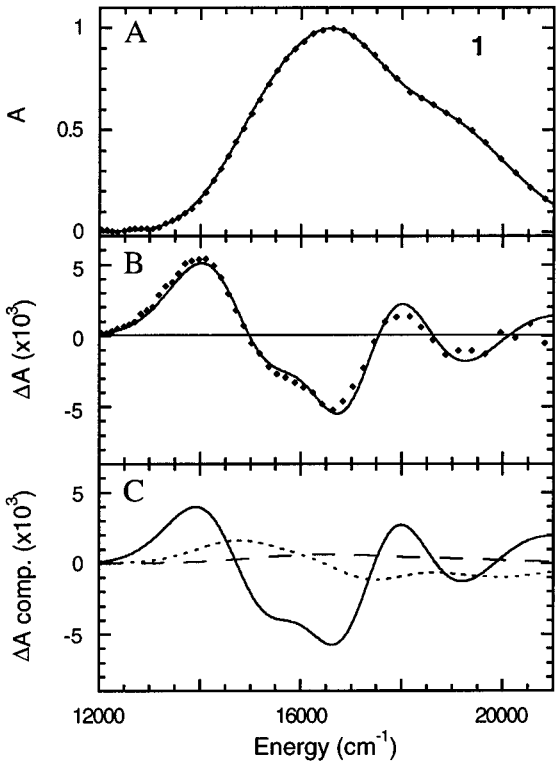

Figure 2. (A) absorption spectrum; (B) Δ*A* (Stark) spectrum of **1** at 77 K in a 1:1 acetone:EtOH solvent mixture at $\chi = 90°$. (C) The zeroth (- -), first (- − -), and second (—) derivative components of the simultaneous best fit to the *A* and Δ*A* spectra. For the absorption and Δ*A* spectrum both data (◆) and fit (—) are shown. All spectra were scaled to a field strength of 1×10^6 V·cm^{-1} and a peak absorbance of unity. The actual sample had an optical density of 0.03.

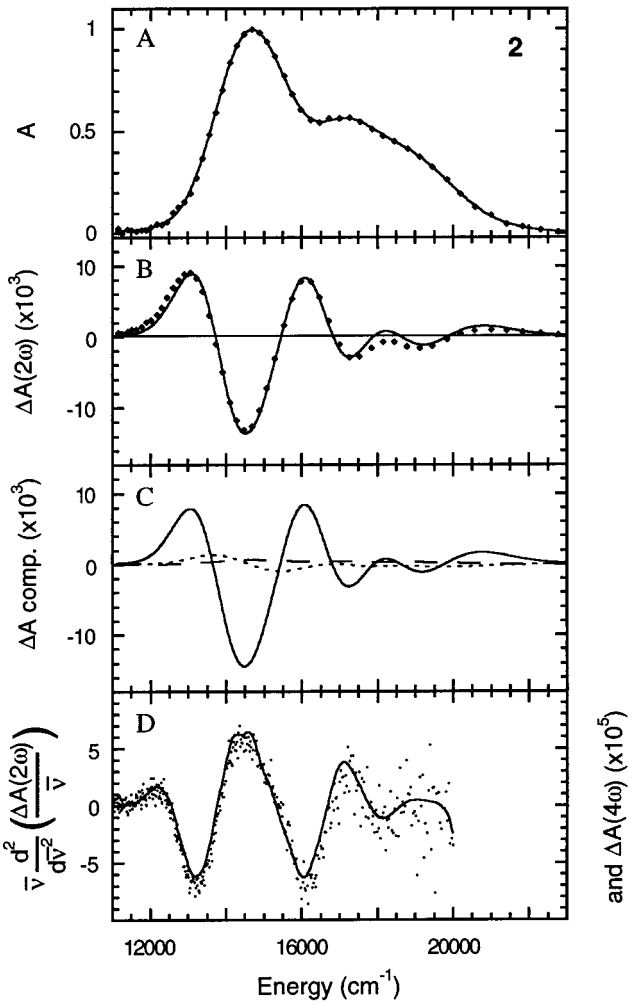

Figure 3. (A) absorption spectrum; (B) conventional (2ω) Stark spectrum of **2** at 77 K in a 1:1 acetone:EtOH solvent mixture at $\chi = 90°$. (C) The zeroth (- -), first (- − -), and second (—) derivative components of the simultaneous best fit to the *A* and 2ω-Stark spectra. For the absorption and 2ω-Stark spectrum both data (◆) and fit (—) are shown. (D) 4ω-HOSS (•••) and scaled $\bar{\nu}$-weighted second derivative of the conventional (2ω) Stark spectrum (—). The Stark spectra were scaled to a field strength of 1×10^6 V·cm^{-1} by using the F^4 (HOSS) and F^2 (2ω-Stark) dependence. The absorption and 2ω-Stark spectrum were scaled to a peak absorbance of unity. The actual sample had an optical density of 0.23. The derivative of the 2ω-Stark spectrum shown in the bottom panel was multiplied by a factor of 6060, corresponding to a value of $f \cdot |\Delta\mu| = 24.5$ D (assuming $\zeta_A = 0°$, cf. eq 7).

approximately parallel. This is expected for a MMCT transition,[9] and values of $|\Delta\mu|$ reported in Table 1 were calculated from the data assuming $\zeta_A = 0°$.

Compound **1** (cf. Figure 2) exhibits a broad absorption band peaked at about 16 750 cm^{-1} with a shoulder at approximately 18 000 cm^{-1}. The line shape of the Stark spectrum is dominated by the second derivative component (cf. panel C, Figure 2) with only minor contributions from the first and zeroth derivative components. The best fit maps the experimental spectrum quite well with slightly larger deviations between data and model at higher energies. The result of the best fit translates into a large difference dipole moment of $f \cdot |\Delta\mu| = 21$ D and a moderately large polarizability change of $f^2 \cdot \mathrm{Da} = 550$ Å^3.

The results for compounds **2** (cf. Figure 3) and **4** (cf. Figure 5) are very similar. Two broad overlapping bands with a peak separation >3000 cm^{-1} can be clearly distinguished in the absorption spectra. For **2** the higher energy band is clearly composed of two components, as shown by the presence of a shoulder at ~19 000 cm^{-1}. Similar to compound **1**, for both **2** and **4** the 2ω-Stark spectrum is dominated by a second derivative line shape with only small first and zeroth derivative contributions. The fitting components translate into values of $f \cdot |\Delta\mu| =$ 23 and 24 D as well as $f^2 \cdot \mathrm{Da} = 400$ and 525 Å^3 for **2** and **4**, respectively. The agreement between data and fit is again quite good with a slightly larger discrepancy at higher energies. For both compounds the HOSS and the $\bar{\nu}$-weighted second derivative of the 2ω-Stark spectrum match across the entire spectrum, using a scaling factor for the derivative spectrum (cf. eq 7) that translates to $f \cdot |\Delta\mu| = 24.5$ and 22 D for **2** and **4**, respectively. The experimental 2ω-Stark spectrum of **4** matches the previously reported spectrum in line shape and magnitude;[17] however, these authors extracted very different values of $\Delta\mu$ as discussed below.

The absorption spectrum of compound **3** (cf. Figure 4) is broad and unstructured. As for the other compounds, the 2ω-Stark spectrum of **3** has a dominant second derivative line shape; however, the first derivative contribution is slightly larger than for the other compounds. Agreement between the data and fit is very good, and the derivative parameters translate into values of $f \cdot |\Delta\mu| = 28$ D and $f^2 \cdot \mathrm{Da} = 1000$ Å^3. The line shape of the HOSS and $\bar{\nu}$-weighted second derivative of the 2ω-Stark spectrum match well; the scaling factor for the derivative spectrum (cf. eq 7) translates to $f \cdot |\Delta\mu| = 31$ D.

Discussion

The measured $|\Delta\mu|$ values for compounds **1**−**4** correspond to effective charge transfer distances of approximately 90/f %,

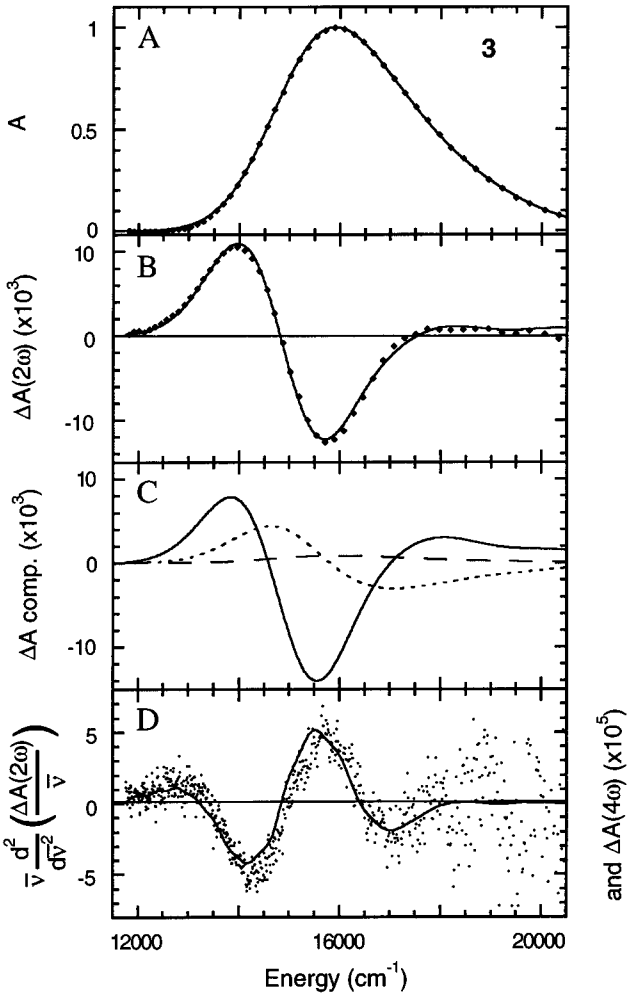

Figure 4. (A) absorption spectrum; (B) conventional (2ω) Stark spectrum of **3** at 77 K in a 1:1 acetone:EtOH solvent mixture at $\chi = 90°$. (C) The zeroth (- -), first (- − -) and second (—) derivative components of the simultaneous best fit to the *A* and 2ω-Stark spectra. For the absorption and 2ω-Stark spectrum both data (◆) and fit (—) are shown. (D) 4ω-HOSS (•••) and scaled $\bar{\nu}$-weighted second derivative of the conventional (2ω) Stark spectrum (—). The Stark spectra were scaled to a field strength of 1×10^6 V·cm^{-1} by using the F^4 (HOSS) and F^2 (2ω-Stark) dependence. The absorption and 2ω-Stark spectrum were scaled to a peak absorbance of unity. The actual sample had an optical density of 0.08. The derivative of the 2ω-Stark spectrum shown in the bottom panel was multiplied by a factor of 9575, corresponding to a value of $f \cdot |\Delta\mu| = 31$ D (assuming $\zeta_A = 0°$, cf. eq 7).

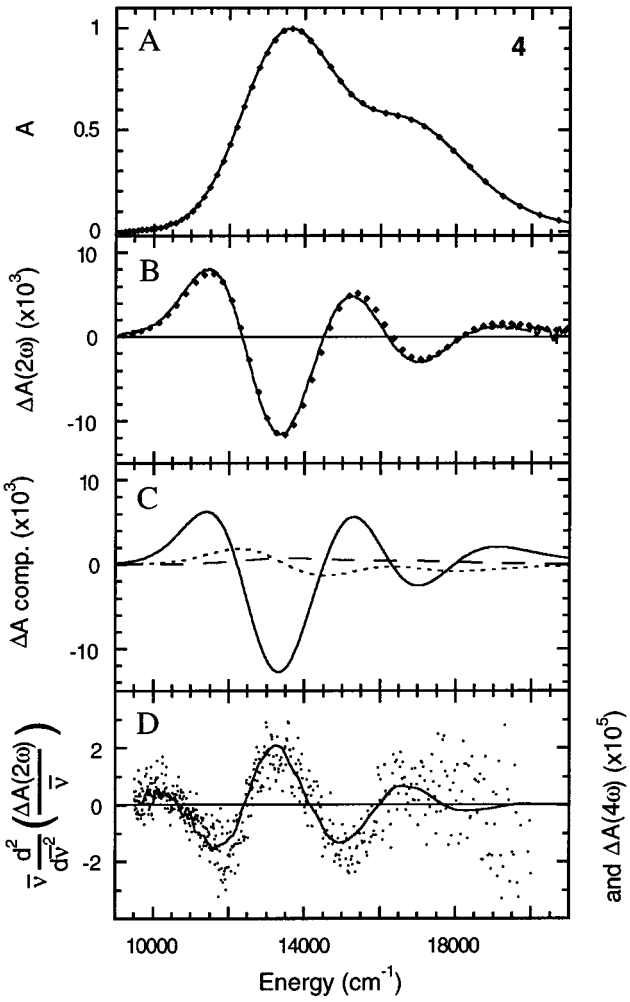

Figure 5. (A) absorption spectrum; (B) conventional (2ω) Stark spectrum of **4** at 77 K in a 1:1 glycerol:water solvent mixture at $\chi = 65°$. (C) The zeroth (- -), first (- − -), and second (—) derivative components of the simultaneous best fit to the *A* and 2ω-Stark spectra. For the absorption and 2ω-Stark spectrum both data (◆) and fit (—) are shown. (D) 4ω-HOSS (•••) and scaled $\bar{\nu}$-weighted second derivative of the conventional (2ω) Stark spectrum (—). The Stark spectra were scaled to a field strength of 1×10^6 V·cm^{-1} by using the F^4 (HOSS) and F^2 (2ω-Stark) dependence. The absorption and 2ω-Stark spectrum were scaled to a peak absorbance of unity. The actual sample had an optical density of 0.16. The derivative of the 2ω-Stark spectrum shown in the bottom panel was multiplied by a factor of 6015, corresponding to a value of $f \cdot |\Delta\mu| = 22$ D (assuming $\zeta_A = 0°$, cf. eq 7).

100/*f* %, 120/*f* %, and 95/*f* %, respectively, of the full metal−metal separation (between 5.0 and 5.2 Å[14,17,18]). The exact value of the local field correction factor, *f*, is not known but is likely to be similar for similar compounds in the same solvent.[11] The previously reported $|\Delta\mu|$ value for $[(NC)_5Fe^{II}\text{-}CN\text{-}Os^{III}(NH_3)_5]^-$ corresponds to about 65/*f* % of the metal−metal separation distance.[16]

One possible reason for an effective charge-transfer distance of less than 100% of the metal−metal separation distance is the presence of ground state charge delocalization. Hush theory is commonly used to estimate the ground state delocalization coefficient, α. Using H_{ab} from eq 1 with r_{ab} set to the metal−metal separation distance, α can be calculated as $\alpha = H_{ab}/\bar{\nu}_{max}$. For compounds **1**−**4** this predicts only about 1% ground state delocalization (using typical values of $r_{ab} = 5.2$ Å, $\bar{\nu}_{max} = 15000$ cm^{-1}, $\epsilon_{max} = 3000$ cm^{-1}·M^{-1}, and $\bar{\nu}_{1/2} = 3500$ cm^{-1}). Alternatively, the ground state delocalization can be calculated from electrochemical data.[26] This method yields values 3−5 times larger than those obtained from Hush theory. For $[(NC)_5Fe^{II}\text{-}CN\text{-}Os^{III}(NH_3)_5]^-$ it predicts that 10% of an electronic charge is transferred in the ground state,[27] which can partially account for the observed small effective charge-transfer distance for this complex. However, since the ground state delocalization, assessed by the Hush method, for compounds **1**−**4** is so small, even the enhancement that could be expected from using electrochemical data is inadequate to account for the observed variations in $\Delta\mu$. In particular the increase in $|\Delta\mu|$ for compound **3** relative to **1**, **2**, and **4** cannot be explained in this way since the optical data indicate a similar extent of delocalization in all four compounds.

Electrostatic effects involving the acceptor group or the spectator ligands of the donor metal ion have been discussed

(26) de la Rosa, R.; Chang, P. J.; Salaymeh, F.; Curtis, J. C. *Inorg. Chem.* **1985**, *24*, 4229−4231.
(27) Dong, Y.; Hupp, J. T. *Inorg. Chem.* **1992**, *31*, 3170−3172.

as another factor that might influence the effective charge-transfer distance.[28−31] The acceptor moiety, $-CN\text{-}Ru^{III}(NH_3)_5$, is the same in this series and obviously cannot account for differences among compounds **1**−**4**; however, the ligands on the donor side are different. It has been suggested that the permanent dipole moment of the spectator ligands can induce a substantial dipole moment along the metal−metal axis.[28,29] The magnitude of this induced dipole moment will depend on the polarizability of the complex. A difference in polarizability, $\Delta\alpha$, then leads to a difference in induced dipole moment between the ground and excited states, thus changing $\Delta\mu$. The importance of this effect has been called into question for MLCT and LMCT processes;[31] however, for MMCT transitions it was argued that this accounts for most of the difference in the expected and observed charge-transfer distance.[28,29] It is important to note that a negative value of $\Delta\alpha$ was assumed in these calculations,[32] while the Stark data show directly that $\Delta\alpha$ is positive for compounds **1**−**4** (cf. Table 1 and refs 16 and 17).

In compounds **1**, **2**, and **4** the spectator ligands can, to a first approximation, be assumed to have a (partial) negative charge in close proximity to the donor metal ion, similar to the charge distribution in the free ligand. However, it is unclear at a quantitative level how the binding affects the charge distribution. In **3** the carbon ligand atom attached to the metal center likely carries a partial positive charge. Although molecular CO carries a partial negative charge on the carbon atom, in CO bound to a metal surface the charges are reversed and correspond to the electronegativity of the atom.[33,34] Since $\Delta\alpha$ is observed to be positive for all mixed valence transitions in **1**−**4**, the ligand dipoles will lead to a direction of $\Delta\vec{\mu}_{ind}$ opposite to that of $\Delta\vec{\mu}_{MMCT}$ for **3** but in the same direction for the other three compounds. The effective charge-transfer distance thus should increase for **2**, **3**, and **4** but decrease for **3**—exactly opposite from the observed differences in $|\Delta\mu|$. Thus, to the extent that these qualitative expectations of the charge distributions in the ligands are valid, it appears that ligand-induced dipole moments cannot account for the observed differences between complexes **1**−**4**.

A more plausible effect which could account for the differences in effective charge-transfer distances is the flow of charge to the donor metal atom from its ligands, in response to the MMCT. A related phenomenon occurs in $[M(bpy)_3]^{3+}$ complexes (M = Zn, Fe, Ru, Os), where it has been shown that nominally ligand-centered transitions in the near-ultraviolet can exhibit large $|\Delta\mu|$ values even though the isolated ligand itself exhibits, as expected, little $|\Delta\mu|$.[35] In these systems the effect has been attributed to the mixing of ligand-centered states with the MLCT state. In the present compounds, if the donor environment is approximately octahedral, as in compounds **3** and **4**, the ligand-to-metal charge flow that accompanies MMCT induces a dipole in the axial CO or CN^- ligand−metal bond relative to the ground-state charge distribution. This can increase $|\Delta\mu|$ beyond what would be expected in the case where the charge is completely localized on the metal atoms. It is clear from the apparent extent of charge transfer that this effect is more important in the $(CO)_5Cr-$ than in the $(CN)_5Os-$ unit. Calculations show that the net charge donation from each CN^- ligand to the osmium atom in the ground state is 0.80 e^-, but that only 0.28 e^- is donated from each of the CO ligands to Cr (J. Waite, private communication). The implication is that back-donation from the filled set of d_π orbitals on the donor metal is much more significant in the $(CO)_5Cr-$ unit. This result is consistent with the low formal oxidation state of chromium. Since a hole is opened in the d_π orbitals during MMCT, there should be a large decrease in back-donation from the chromium atom in the excited state that corresponds to an additional axial component to $|\Delta\mu|$.

Spin−Orbit States. Two peaks separated by more than 3500 cm^{-1} are observed in the absorption spectrum of compound **4**. These are caused by the spin−orbit splitting in the excited state of the donor metal atom (see Appendix). In an octahedral site, a $^2T_{2g}$ (t_{2g}^5) state is split by $^3/_2\zeta$, where ζ is the spin−orbit coupling constant. The lower energy (Γ_7) component at an energy of $-\zeta$ is a Kramers doublet, but the higher one (Γ_8) at $+\ ^1/_2\zeta$ retains a degeneracy that can be resolved in lower symmetry (including axial) fields. EPR data on related ammine complexes can be analyzed by using $\zeta = 2750$ cm^{-1} for Os(III)[36] and $\zeta = 1000$ cm^{-1} for Ru(III) compounds.[37] Thus, assuming that the deviation from octahedral symmetry at the osmium atom is not large, the observed splitting in **4** is of the correct magnitude, as is the roughly 2:1 relative intensity ratio of the components (see Appendix). As expected, compound **2** shows a splitting of similar size, but here the low site symmetry causes the removal of the residual degeneracy to give three component levels.[18] The smaller spin−orbit coupling constant of Ru(III) leads to a more poorly resolved high-energy component in the absorption spectrum of compound **1**. Similarly ζ for chromium(I) is too small to cause any detectable splitting in the spectrum of **3**.

On the basis of their analysis of the Stark spectrum of **4**, Karki and Hupp concluded that there is a significant difference in the effective charge-transfer distance for the two spin−orbit bands, $3.7/f$ eÅ for the lower and $5.3/f$ eÅ for the higher energy band.[17] By contrast, our analysis of the identical experimental data suggests that the effective charge-transfer distances are identical. Karki and Hupp rationalized their finding in terms of the different orientation of the orbitals involved in the two absorption transitions. The lower energy absorption band of **4** was assigned to a transition originating from a degenerate pair of Os 5d-orbitals partially aligned along the charge-transfer axis. The higher energy band is believed to involve a single Os 5d-orbital that is nominally orthogonal to the charge-transfer axis but becomes allowed through asymmetries in the ligand field and through mixing of the d-orbitals via spin−orbit coupling.[17] However, judging from the absorption data, the spin−orbit interaction is the dominant interaction, since the separation of the two bands is comparable with that due to that perturbation alone in an octahedral site (see Appendix). Any axial field perturbation must be diagonalized simultaneously with the spin−orbit interaction. The dominance of the latter means that it is misleading to associate the eigenvectors with particular spatial components of the t_{2g} orbitals, as suggested by Karki and Hupp.

(28) Reimers, J. R.; Hush, N. S. In *Mixed Valency Systems: Applications in Chemistry, Physics and Biology*; Prassides, K., Ed.; Kluwer Academic: Dordrecht, 1991; pp 29−50.
(29) Reimers, J. R.; Hush, N. S. *J. Phys. Chem.* **1991**, *95*, 9773−9781.
(30) Shin, Y. K.; Brunschwig, B. S.; Creutz, C.; Sutin, N. *J. Am. Chem. Soc.* **1995**, *117*, 8668−8669.
(31) Shin, Y. K.; Brunschwig, B. S.; Creutz, C.; Sutin, N. *J. Phys. Chem.* **1996**, *100*, 8157−8169.
(32) A two-level model which considers only the ground state and first excited state will always predict $\Delta\alpha$ to be negative.
(33) Surnev, L.; Xu, Z.; Yates, J. T. J. *Surf. Sci.* **1988**, *201*, 14−26.
(34) J. T. Yates, Jr. Personal communication.
(35) Hug, S. J.; Boxer, S. G. *Inorg. Chim. Acta* **1996**, *242*, 323−327.
(36) Medina, A. N.; Gandra, F. G.; Lima, J. B.; McGarvey, B. R.; Franco, D. W *J. Chem. Soc., Faraday Trans.* **1997**, *93*, 2105−2111.
(37) Blake, A. B.; Delfs, C. D.; Engelhardt, L. M.; Figgis, B. N.; Reynolds, P. A.; White, A. H.; Moubaraki, B.; Murray, K. S. *J. Chem. Soc., Dalton Trans.* **1993**, 1417−1420.

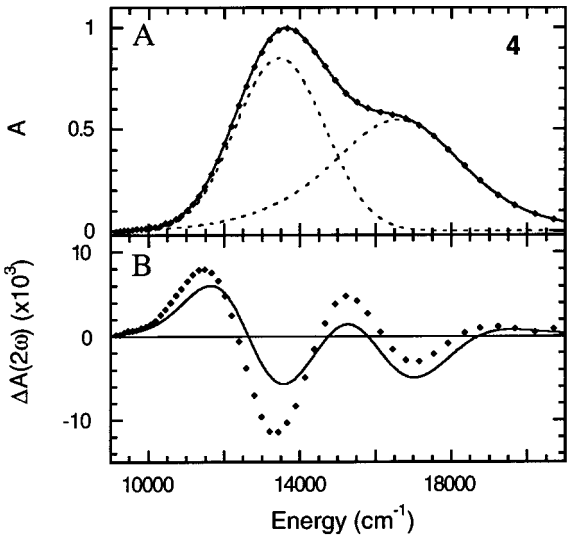

Figure 6. (A) absorption spectrum; (B) 2ω-Stark spectrum of **4** at 77 K in a 1:1 glycerol:water solvent mixture at $\chi = 65°$. For each spectrum both data (◆) and model (—) are shown. In panel A the model of the two individual absorption bands is shown as well (- − -). The model of the Stark spectrum shown in panel B uses the $\Delta\mu$ and $\Delta\alpha$ values previously reported by Karki and Hupp[17] for **4**, $f \cdot |\Delta\mu| = 17.7$ and 25.5 D and $f^2 \cdot \mathrm{Da} = 975$ and 1550 Å^3 for the lower and higher energy band, respectively. The zeroth derivative components of the model were fixed at zero—see text. It is evident that the fit is poor (compare Figure 4B); a good fit can only be obtained by including oppositely signed and unrealistically large zeroth derivative components.

The Appendix shows that, providing the degree of metal-to-metal delocalization is small, the two excited states should not therefore differ significantly in their effective charge-transfer distances, in agreement with our finding that $|\Delta\mu|$ (and $\Delta\alpha$) is nearly identical for these two bands (Table 1). Likewise, for compound **2** the agreement between the data and fit is very good across the entire spectrum when only a single value of $|\Delta\mu|$ and $\Delta\alpha$ is used. Fits of the ΔA spectra of **2** and **4** when more than one set of derivative parameters are used (carefully avoiding the introduction of artifacts[12]) did not result in any significant difference of the $\Delta\mu$ values for the different bands. The homogeneity of the electronic structure is further confirmed by the HOSS data which for both complexes yield $|\Delta\mu|$ values similar to those obtained from the conventional 2ω-Stark spectra.

In general, it is important to be careful when analyzing Stark data for overlapping bands. To see this clearly for the present case, fits of the A and ΔA data of **4** are shown in Figure 6 by using values reported for $\Delta\mu$ and $\Delta\alpha$ for each spin−orbit band by Karki and Hupp.[17] This model clearly does not match the data (compare the best fits in Figure 4A and B), greatly underestimating ΔA for the lower energy band while overestimating ΔA for the higher energy band. Karki and Hupp reported good agreement between data and model; however, they did not show the decomposition into a sum of derivatives, as in Figure 4C. This good agreement reported by Karki and Hupp can only be obtained if large zeroth derivative components of opposite signs for the two bands accounting for up to 50% of the magnitude of the ΔA data are included in the fit. There is no theoretical justification for this, and it is unnecessary as demontrated by the excellent fit in Figure 4B where the zeroth derivative component contributes less than 5% to the ΔA signal. Generally, an unrestricted fit of the Stark response of overlapping absorption bands using different derivative parameters for each band is prone to the introduction of artificial results due to interfering effects on the two bands.[38] This can be avoided by collecting HOSS data. As outlined above, the analysis of HOSS data with eq 7 does not require any model fitting functions and involves only comparisons among experimental data. This provides a reliable way of determining whether the electronic structure changes across the absorption spectrum. For example, in acceptor-substituted carotenoids large changes in $|\Delta\mu|$ across the absorption band are clearly revealed by HOSS.[12]

Appendix − Intensity of the Spin−Orbit Component Transitions

The zeroth-order wave functions are taken as those of the octahedral t_{2g} shells on the donor and acceptor centers. These two sets of bases can be related by the common C_4 axis along z, i.e., the metal−metal direction. Because spin−orbit coupling is large at both metal centers it is convenient to use spinors that diagonalize this interaction. The one-electron functions are therefore bases for the Γ_7 (E'') and Γ_8 (U′) irreducible representations of O*. In the notation of Griffith[39] these are related to space-spin products by:

$$\mathrm{E}''\alpha'' = \frac{1}{\sqrt{3}}|t_2 0,\alpha\rangle - \frac{\sqrt{2}}{\sqrt{3}}|t_2 + 1,\beta\rangle$$

$$E''\beta'' = \frac{\sqrt{2}}{\sqrt{3}}|t_2 - 1,\alpha\rangle - \frac{1}{\sqrt{3}}|t_2 0,\beta\rangle$$

$$U'\kappa = -\frac{1}{\sqrt{3}}|t_2 - 1,\alpha\rangle - \frac{\sqrt{2}}{\sqrt{3}}|t_2 0,\beta\rangle$$

$$U'\lambda = |t_2 - 1,\beta\rangle$$

$$U'\mu = |t_2 + 1,\alpha\rangle$$

$$U'\nu = \frac{\sqrt{2}}{\sqrt{3}}|t_2 0,\alpha\rangle - \frac{1}{\sqrt{3}}|t_2 + 1,\beta\rangle \qquad (1)$$

In terms of $|LM_L\rangle$ kets and the real d-orbitals, the spatial functions are given by $t_2 0 = 1/\sqrt{2}(|22\rangle - |2\ -2\rangle) = id_{xy}$, $t_2 + 1 = |2\ -1\rangle = -i/\sqrt{2}(d_{yz} + d_{xz})$ and $t_2 - 1 = -|21\rangle = i/\sqrt{2}(d_{yz} - d_{xz})$. α and β are the spin functions.

The one electron spin−orbit energies are $-1/2\zeta$ for U′ and $+\zeta$ for E''. In the ground state there is a hole in the t_{2g} orbitals of the Ru(III) ion, and thus in the E'' spinors which lie ∼1500 cm^{-1} higher in energy than the U′. The ground-state wave functions have E'' symmetry and, in an obvious notation derived from eq 1, are $|\kappa_d\lambda_d\mu_d\nu_d\alpha_d''\beta_d''\kappa_a\lambda_a\mu_a\nu_a\alpha_a''\rangle$ and $|\kappa_d\lambda_d\mu_d\nu_d\alpha_d''\beta_d''\kappa_a\lambda_a\mu_a\nu_a\beta_a''\rangle$, where the subscripts distinguish donor and acceptor functions. The MMCT excited states are obtained by filling the hole in the E“ acceptor shell by a transition from either E” or U′ spinors on the donor. The transition moment operator for axial charge transfer is invariant with respect to C_4(z), so only those transitions where the initial and final states transform identically under this operation are allowed. Thus only $E''\alpha'' \rightarrow E''\alpha''$, $E''\alpha'' \rightarrow \mathrm{U}'\nu$, $E''\beta'' \rightarrow E''\beta''$ and $E''\beta'' \rightarrow \mathrm{U}'\kappa$ contribute to the intensity. The relevant matrix

(38) ΔA for each band can be either positive or negative. For example, a combination of a positive and a negative zeroth derivative component for overlapping bands can lead to a model that resembles the first derivative of the full spectrum.

(39) Griffith, J. S. *The Theory of Transition-Metal Ions*; Cambridge University Press: London, 1961.

elements are:

$$\langle \kappa_d \lambda_d \mu_d \nu_d \alpha''_d \beta''_d \kappa_a \lambda_a \mu_a \nu_a \alpha''_a | e\mathbf{z} | \kappa_d \lambda_d \mu_d \nu_d \alpha''_d \kappa_a \lambda_a \mu_a \nu_a \alpha''_a \beta''_a \rangle =$$
$$\langle \beta''_d | e\mathbf{z} | \beta''_a \rangle = \frac{1}{3}\langle t_2 0(d) | e\mathbf{z} | t_2 0(a) \rangle + \frac{2}{3}\langle t_2 - 1(d) | e\mathbf{z} | t_2 - 1(a) \rangle$$

$$\langle \kappa_d \lambda_d \mu_d \nu_d \alpha''_d \beta''_d \kappa_a \lambda_a \mu_a \nu_a \alpha''_a | e\mathbf{r} | \lambda_d \mu_d \nu_d \alpha''_d \beta''_d \kappa_a \lambda_a \mu_a \nu_a \alpha''_a \beta''_a \rangle =$$
$$\langle \kappa_d | e\mathbf{z} | \beta''_a \rangle = \frac{2}{3}\langle t_2 0(d) | e\mathbf{z} | t_2 0(a) \rangle + \frac{\sqrt{2}}{3}\langle t_2 - 1(d) | e\mathbf{z} | t_2 - 1(a) \rangle \quad (2)$$

with equivalent expressions for the Kramers conjugate states. Matrix elements of the type $\langle \lambda_d | e\mathbf{z} | \beta''_a \rangle$ vanish on spin integration. The first transition moment in eq 2 applies to an $E'' \rightarrow E''$ transition, i.e., to the lower energy of the two excited states, and the second to an $E'' \rightarrow \mathrm{U}'$ transition to the higher energy state.

The bridging cyanide ion has no orbitals available with the same axial symmetry as the $t_2 0$ (d_{xy}) metal functions, so to a very good approximation the overlap integral $\langle t_2 0(d) | t_2 0(a) \rangle$ is zero, and the contribution of the $t_2 0$ orbitals to the transition moment is negligible. The remaining terms in eq 2 are proportional to a transfer integral that originates in superexchange via the π orbitals of the cyanide bridge. Their relative magnitude (i.e. $\sqrt{2}$:1) predicts that the $E'' \rightarrow E''$ transition should have twice the intensity of the $E'' \rightarrow \mathrm{U}'$ transition.

From the coefficients of the $t_2 \pm 1$ orbitals in eq 1 we note that the extent of delocalization in the E'' spinors should be twice as large as that in the $\mathrm{U}'\kappa$ and $\mathrm{U}'\nu$ spinors that contribute to the transition probability. It follows that, if the metal-to-metal delocalization coefficient was in fact much larger than the $\sim$ 1% suggested by the Hush model, $|\Delta\mu|$ would be observably larger in the higher energy $E'' \rightarrow \mathrm{U}'$ transition than in the $E'' \rightarrow E''$ transition.

Finally the influence of an axial perturbation, in which the leading term transforms as $E\theta$, on the octahedral functions at either or both metals, can be determined by examining the appropriate coupling coefficients in O^*, or by inspection of the functions in eq 1. The perturbation operates in second order and leads to a superposition of $E''\alpha''$ with $U'\nu$, and of $E''\beta''$ with $U'\kappa$. These functions share the same E'' irreducible representations of the D_4^* double group. The effect is to split the $U'(O^*)$ spinors into two sets, $E''(D_4^*)$ and $E'(D_4^*)$, of which the former are at lower energy, and to raise the energy of the set stemming from the $E''(O^*)$ spinors. Because of the constraints imposed by axial charge transfer and spin orthogonality, the $E'(D_4^*) \rightarrow E''(D_4^*)$ transitions are forbidden. Consequently there continue to be only two allowed transitions in the presence of the perturbation, but their separation is augmented by the second-order effect of the axial field. The modification to the wave functions implies that the intensities of the two transitions become progressively more equal as the magnitude of the axial field increases. This effect is a composite of the axiality at both metal centers. The constraints on the transition moments are removed when the symmetry is lower than axial, and all three transitions are then allowed. This is clearly the case for compound **2**, where three component transitions are resolved.

Acknowledgment. This work is supported in part by a grant from the National Science Foundation Chemistry Division. W.M.L. is the grateful recipient of an EPSRC Postdoctoral Fellowship.

JA980453S